A versatile shear cell for investigation of structure of food materials under shear

Velichko, Evgenii; Tian, Bei; Nikolaeva, Tatiana; Koning, Jeroen; van Duynhoven, John; Bouwman, Wim G.

DOI
10.1016/j.colsurfa.2018.12.046

Publication date
2019

Document Version
Final published version

Published in
Colloids and Surfaces A: Physicochemical and Engineering Aspects

Colloids and Surfaces A 566 (2019) 21–28

Contents lists available at ScienceDirect

Colloids and Surfaces A

journal homepage: www.elsevier.com/locate/colsurfa

A versatile shear cell for investigation of structure of food materials under shear

Evgenii Velichko[a,*], Bei Tian[a,1], Tatiana Nikolaeva[b,1], Jeroen Koning[c], John van Duynhoven[b,d], Wim G. Bouwman[a]

[a] Department of Radiation Science & Technology, Delft University of Technology, Mekelweg 15, 2629JB Delft, The Netherlands
[b] Laboratory of Biophysics, Wageningen University, Stippeneng 4, 6708WE Wageningen, The Netherlands
[c] Electronic and Mechanical Support Division, Delft University of Technology, Mekelweg 15, 2629JB Delft, The Netherlands
[d] Unilever R&D, Olivier van Noortlaan 120, 3133 AT Vlaardingen, The Netherlands

GRAPHICAL ABSTRACT

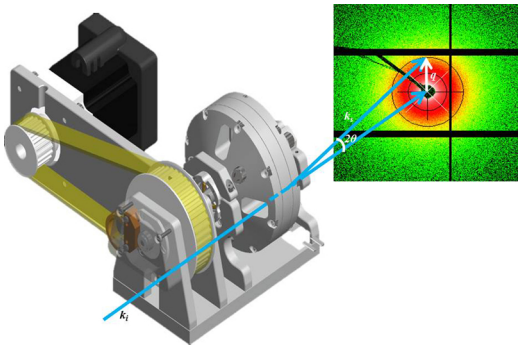

ARTICLE INFO

Keywords:
Shear-SAXS
Shear-SANS
Food colloids
Food mesostructure
Food texture

ABSTRACT

A versatile cell for X-ray and neutron scattering experiments on samples under shear has been designed. To our knowledge, it is the first shear cell which can be used for both SAXS and SANS in respectively synchrotron or reactor beamlines. The cell is mainly intended for scattering experiments in so-called "1–2 plane geometry", but can also be modified into cone–plate and plate–plate rheological geometries, giving access to the 1–3 scattering plane. The latter two geometries, however, can only be used with neutron scattering. The final cell design is compact, which allows it to be used even with lab-based X-ray sources. A special thermostatic shell allows for the temperature control of the samples under investigation in the range from 5 up to 100 °C. Several X-ray and neutron scattering experiments performed with the cell have helped in better understanding of the structuring under shear of food materials, such as: cellulose suspensions, fat crystal networks and milk proteins.

1. Introduction

A major challenge for food science is to reconcile the societal drive towards sustainable food production with the consumers demand for natural, stable and superior tasting foods [1]. Conventional routes for food manufacturing have been optimized over decades and have

* Corresponding author.
E-mail address: e.velichko@tudelft.nl (E. Velichko).
[1] These authors contributed equally to this work.

https://doi.org/10.1016/j.colsurfa.2018.12.046
Received 15 October 2018; Received in revised form 22 December 2018; Accepted 22 December 2018
Available online 29 December 2018

reached their limits. The required radical redesign of food formulation and processing routes requires deepened insights in relationships between product structure and functionality [2]. When processing raw materials to final consumer food products, their structures undergo changes at multiple length scales [3,4]. A prerequisite for rational redesign of food processing routes is to have insights in how these hierarchical multiscale structures evolve under dynamic condition [3].

Small-angle scattering (SAS) of X-rays (SAXS) and neutrons (SANS) is widely utilized to study structures of food colloids [5–10]. A number of works has also been done on application of these techniques on materials under shear or flow conditions [11,12]. Both methods, SAXS and SANS [13] are capable of investigations on nano- and mesoscale size range, moreover, by utilizing a spin-echo principle for SANS encoding (SESANS [14]), the range can be extended up to 20 μm. However, these methods have certain advantages and disadvantages related to the employed type of radiation. X-rays interact with electron clouds of atoms, which leads to linear dependency of scattering power on the atomic number of the element. Neutrons interact with atom nuclei, which causes different scattering power for different isotopes of the same chemical element. This effect is widely employed in experiments with contrast variation. Moreover, due to the weak interaction of neutrons with matter, rather bulky samples can be studied with neutron scattering. Since X-rays are easy to generate, a multitude of laboratory-scale plug-and-play SAXS instruments came to the market in recent years. Compact neutron sources are still under development and SANS experiments still require large-facilities like nuclear reactors, or spallation sources. Synchrotrons, large-facilities generating X-ray are also open for SAXS experiments. One of the great advantages of synchrotrons is their high flux of X-rays, which is 6–7 orders of magnitude higher than average flux of neutrons at neutron large-facilities. Such a high flux allows for a very high time resolution, as well as high spatial resolution of the experiment, as X-ray beam at synchrotron can easily be focused to 100 μm, or, with special optics, even to a few nm. However, such high flux might be a considerable disadvantage in studies of soft matter, as samples can easily get radiation damage or even destroyed within a fraction of a second. Taking into account compatibility of X-rays and neutrons, we decided to make our shear-cell suitable for both kind of radiation, so that we could perform (SE)SANS and SAXS experiments on complex fluids under the same conditions. In the following the cells, suitable for either SANS or SAXS on the samples under shear, will be called shear-SAS cells.

Table 1 gives an overview of the shear-SAS cells described in the literature. As can be seen, the most popular cell geometry is Taylor–Couette, which allows for radial and tangential passage of the beam

Table 1
Shear-SAS cells described in the literature.

Source	Simultaneous torque measurement	Type of radiation	Cell geometry	Scattering plane(s)
[23]	–	Neutrons	Taylor–Couette	1–3
[24]	–	Neutrons	Taylor–Couette	1–3
[25]	–	neutrons	Taylor–Couette	1–3
[26]	–	Neutrons	Taylor–Couette	1–3
[27]	–	X-rays	Plate–plate	1–2
[28]	–	Neutrons	Poiseuille	1–2
[29]	–	Neutrons	Plate–plate	1–2
[30]	–	Neutrons	Plate–plate	1–3
[31]	–	X-rays	Taylor–Couette	1–3, 2–3
[32]	–	X-rays	Cone–plate	1–2
[33]	–	Neutrons	Taylor–Couette	1–2
[15]	+	X-rays	Taylor–Couette	1–3, 2–3
[17,18]	–	Neutrons	Taylor–Couette	1–2
[16]	+	Neutrons	Taylor–Couette	1–3, 2–3
[34]	+	X-rays	Plate–plate	1–3
[35]	+	Neutrons	Taylor–Couette	1–3, 2–3
[36]	+	X-rays	Sliding plate	1–2
[37]	+	Neutrons	Taylor–Couette	1–3, 2–3

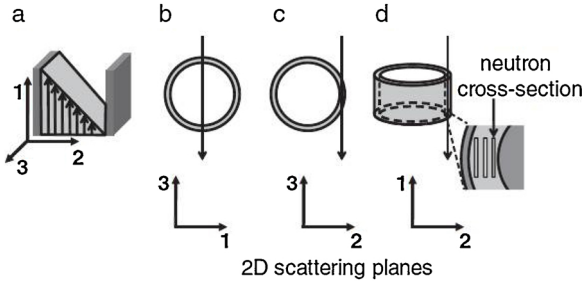

Fig. 1. The common Taylor–Couette flow cell geometries with accessible scattering planes. (a) Rectilinear coordinate frame where the 1-, 2-, and 3-directions are defined as the velocity (V), velocity gradient (ΔV), and vorticity (ω) directions, respectively. (b), (c), and (d) are the radial, tangential, and 1–2 plane flow cell geometries that allow for scattering along the 1–3, 2–3, and 1–2 planes, respectively. In the latter, an incident beam cross-section smaller than the fluid gap allows for spatial resolution along the gap. The figure is adopted from [12].

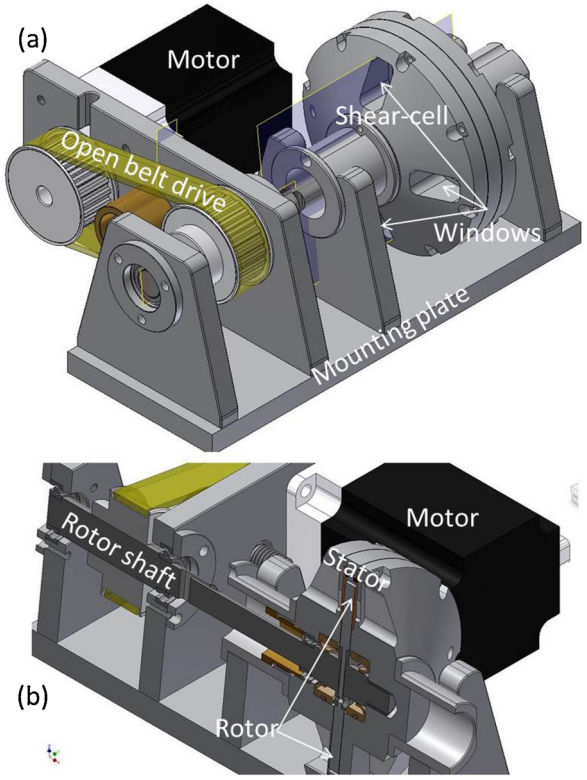

Fig. 2. A schematic 3D drawing of the developed shear-cell (a) and a vertical cross section of it along the rotation axis of the cell (b).

along the cell (for more details of various cell geometries as well as scattering planes see the review [12]). Depending on the direction of the beam relative to the shear cell, three different scattering geometries are possible. Fig. 1 shows three possible scattering geometries based on the Taylor–Couette cell. AntonPaar was the first company able to combine a rheometer with a suitable Taylor–Couette cell with small-angle scattering of X-rays [15], a few years later simultaneous SANS and torque measurements were performed with a rheometer of Rheowis-Fluid (Labplus, Jona, Switzerland) [16]. Another way of evolution of shear-SAS cells was a development of so-called “1–2 plane shear cell” [17,18]. As such a cell allows spatial resolution along the shear-gradient direction across the gap, it is very attractive for investigation of materials showing shear-banding [17,19–22]. However,

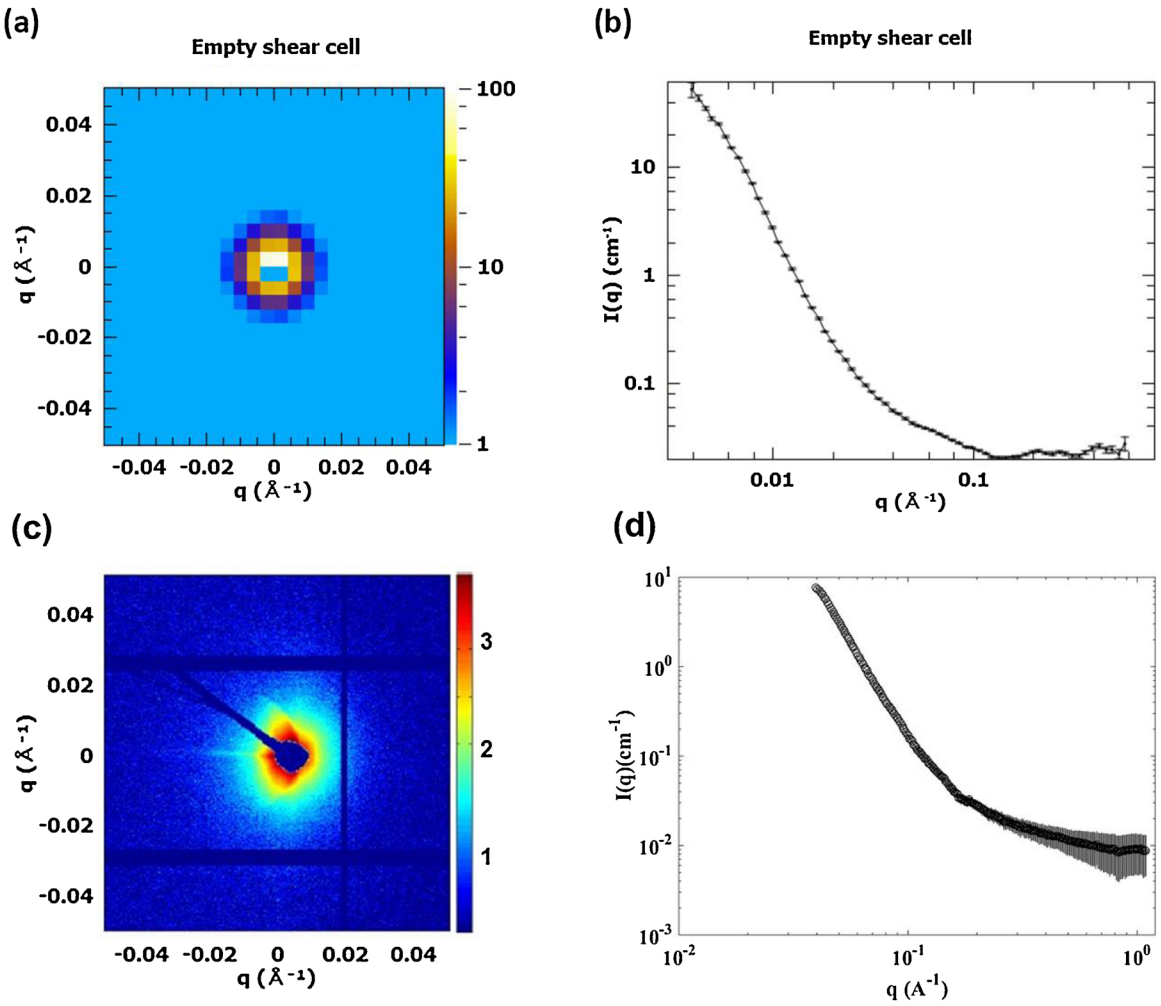

Fig. 3. 2D (a) and 1D (b) SANS patterns from the empty shear cell in cone–plate configuration. 2D (c) and 1D (d) SAXS patterns from the empty shear cell in Taylor–Couette cell geometry. The scattering was collected at LARMOR beamline of ISIS neutron source (a and b) and at BM26 (DUBBLE) beamline of ESRF (c and d).

this geometry does not allow for a simultaneous torque measurement, as the cell is placed horizontally, while all of the existing rheometers are vertical. For our design we decided to omit possibility for a simultaneous torque measurement and chose for horizontal cell geometry.

In this article we present detailed design of the versatile shear-cell suitable for SAXS, SANS and SESANS measurements. Three examples of shear-SAS cell application for studies of food colloids are presented in the experimental section. Although in our research we focused mostly on application of the shear-SAS cell for investigation of food colloidal dispersions, the applications can be extended to the much broader field of soft matter.

2. Apparatus

Fig. 2 shows a schematic drawing of the developed shear-SAS cell and Fig. A.9 shows an image of the cell mounted at the SAXS DUBBLE (BM-26) beamline at ESRF [38,39]. As can be seen from Fig. A.9, the cell with its drive and motor is rather compact (it can fit in a box of $25 \times 25 \times 25\,cm^3$), which makes it easy in transportation, it even has been transported as hand luggage on an airplane. The compactness made it possible to mount it on various beamlines and even laboratory X-ray sources (see Section 3.1). The cell consists of an inner rotating disk (rotor) and an outer stable container (stator), leaving a gap which is filled up with the material under investigation. Rotor and stator are both made of aluminum.

2.1. Fit for neutrons and X-rays

In order to make the cell suitable for X-rays and neutrons, special types of windows were necessary for each type of radiation. In case of neutrons 0.4 mm thick aluminum windows with accessible area $10 \times 17\,mm^2$ are integrated in the cell design. Fig. 3 shows a 2D (a) and 1D (b) SANS patterns from the empty shear cell. For X-rays two circular diamond windows with 0.2 mm thickness and 6 mm diameter were created, which give hardly any background scattering (see Fig. 3(c) and (d)). For visual inspection of the sample and potential light scattering applications, 1 mm thick quartz windows with accessible area $8 \times 15\,mm^2$ were added to the cell design. Fig. A.10 shows the windows positions on the cell. It should be noted, that in order to obtain the most homogeneous sample flow at the measurement position, the cell should be positioned in such a way that required window appears on the side of the cell (in Fig. A.10(a) quartz and diamond windows are in the right position).

As the cell is also intended to be used for SESANS measurement, we had to minimize magnetic fields appearing due to motor driving the cell. At the current distance between the aluminum window of the cell and the motor (20 cm) we did not observe any effects of the motor magnetic field on the neutron beam polarization.

2.2. Shear-SAS cell geometries

The cell is mainly intended to probe the so-called 1–2 scattering

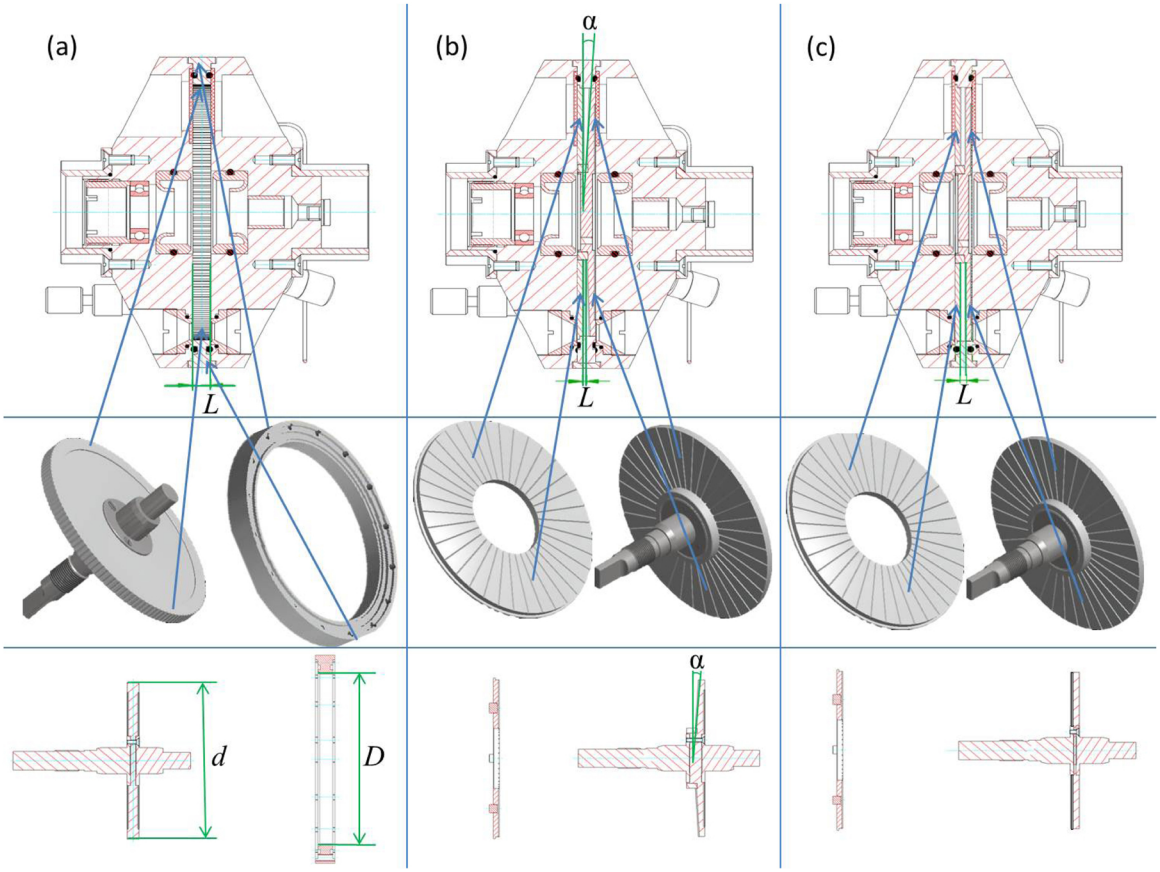

Fig. 4. Geometries of the cell: (a) Taylor–Couette geometry, (b) cone–plate geometry, and (c) plate–plate geometry. The top row shows a cross section of the entire cell, the stators and rotors for respective geometries are shown in the middle row with their respective cross sections in the bottom row. Blue arrows show where the stators and rotors appear on the drawings of the cross sections. L is a sample thickness on the beam, d is a diameter of the rotor, D is an inner diameter of the housing ring, and α is the cone angle.

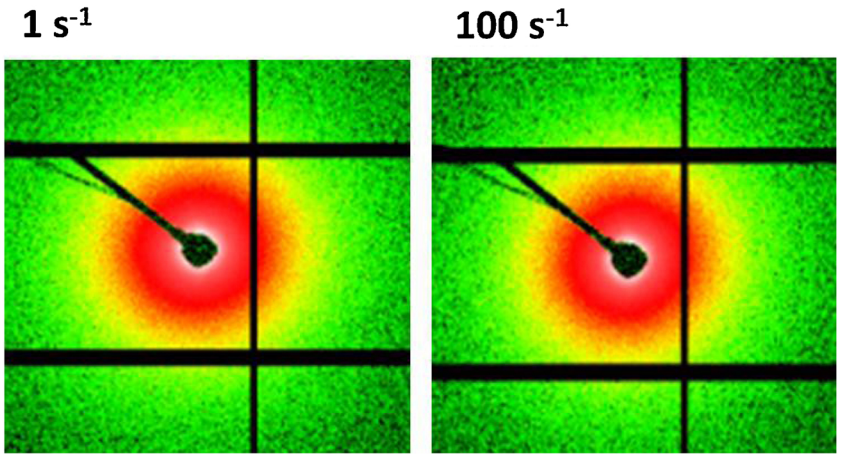

Fig. 5. 2D SAXS patterns for a sample of microfibrillated bacterial cellulose (BC) with carboxymethylcellulose (CMC) with a concentration of BC 0.2 wt%. and ratio BC:CMC = 4:1 at 1 (left) and 100 (right) s^{-1}. The patterns are shown for a point in the middle of the cell gap.

plane of the complex fluids. The Taylor–Couette cell geometry for this application is similar to one described in [18] with the additional possibility for the SAXS experiments. This geometry in combination with intensive neutron or X-ray beam allows for spatially-resolved SAXS/SANS measurements across the gap. Moreover, since the cell is made of aluminum, which is relatively transparent for neutrons, we decided to use this advantage and extend the cell design to two more geometries, namely cone–plate and plate–plate. All three geometries are shown in Fig. 4.

In the Taylor–Couette geometry, the shear-SAS cell allows access to so-called 1–2 scattering plane, which in combination with intensive beams allows for spatially-resolved SAXS/SANS measurements across the gap. Therefore, it is possible to locally probe structure of the material under investigation. By varying thicknesses of the rotor and outer ring, it is possible to achieve different sample thicknesses along the beam L. However, the minimal value of L is 4 mm due to mechanical limitations. The gap size between the rotor and the ring also can be varied by varying the rotor diameter d. In our experiments we were

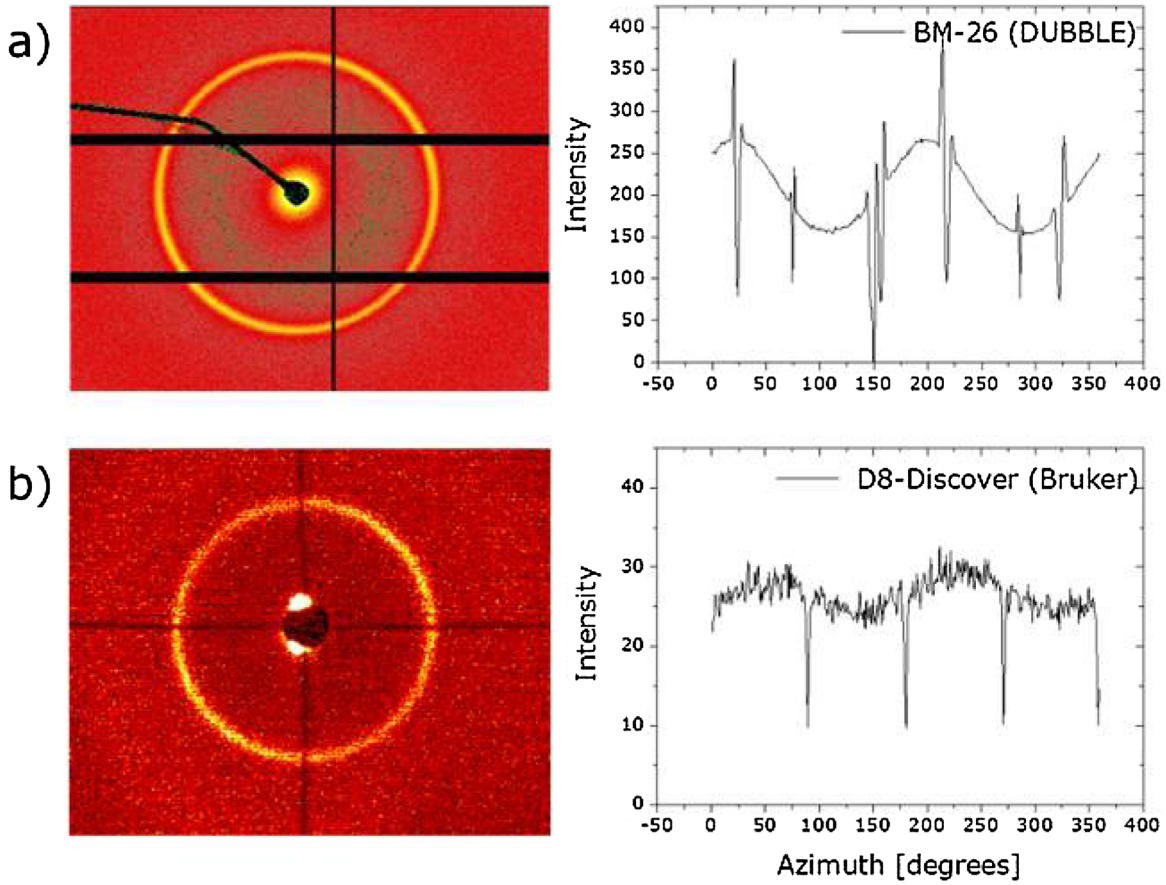

Fig. 6. 2D SAXS patterns and their radial averages presented in the intensity vs Azimuth angle plots for MFC nanoplatelets dispersed in sunflower oil obtained at the BM-26 (DUBBLE) beamline at ESRF (a) and at the lab-scale Bruker D8-Discover X-ray diffractometer (b). Both experiments were performed in the developed Couette geometry with serrated walls at an imposed shear rate of 0.1 s^{-1} and ambient temperatures.

using a gap size of 1 mm. It can be increased up to 6 mm for X-ray experiments and up to 15 mm for experiments with neutrons.

In plate–plate or cone–plate geometry the scattering pattern appears in 1–3 scattering plane. In this case the beam is going through the sample along the shear-gradient direction and the scattering pattern is integrated over all shear rates present in the system. In this case the sample thickness along the beam can be varied either by changing the thickness of the rotor or by changing the cone angle α. The cone angle can be varied between 1° and 10°. In our experiments we were using $\alpha = 3°$.

In all three geometries, the surfaces of the rotor and the stator can be made smooth, sand-blasted, or serrated, depending on roughness desired for the planned experiment.

2.3. Temperature control

Since rheology and structure of food is highly dependent on temperature and temperature history of the material, we included a special housing for temperature control of the cell in our design. A thermostatic shell was designed for this purpose. The shell is made of 1 mm thick nylon 12 with copper insertions for better temperature exchange. The nylon parts of the cell were 3D-printed and the copper insertions were glued to them with a temperature-resistant glue. The internal surface of the shell follows the shape of the shear cell and has maximal available contact surface area with the cell. The shell is hollow, which allows for the flow of a cooling or heating liquid with desired temperature through it. For temperature measurements a K-type thermocouple is used. Fig. A.11 shows a cross section of the cell in the thermostatic shell as well as the internal surface of the shell with copper insertions.

3. Experimental results and discussion

A couple of in-situ experiments were conducted so far: one at the DUBBLE beamline at ESRF [38,39] and one at the LARMOR instrument at ISIS. In the first case the Taylor–Couette geometry was used in combination with X-ray scattering for investigation of cellulose dispersions and fat crystal dispersions. In the second experiment protein dispersions were studied in plate–plate and cone–plate geometry with aid of neutron scattering.

3.1. X-rays: microfibrillated cellulose dispersions

So-called non-local flow behaviour of microfibrillated cellulose was observed by Rheo-MRI [40]: the viscosity of the sample was dependent on the position across the cell gap. This can be explained by a formation of flocks of microfibrills, or a formation of an aligned liquid crystal phase.

In order to check these two models, we have performed a shear-SAXS experiment at the BM-26 (DUBBLE) beamline at ESRF [45]. Fig. 5 shows typical scattering patterns for a sample of microfibrillated bacterial cellulose stabilized by carboxymethylcellulose (BC-CMC) at high and low shear rates. The scattering patterns appear to be isotropic at both shear rates. This result indicates absence of aligned liquid crystal phase, and sustains the flocculation model as the explanation for the position dependent viscosity.

3.2. X-rays: in situ view on fat crystal network formation

Stability and sensorial quality of fat-based products, such as butter

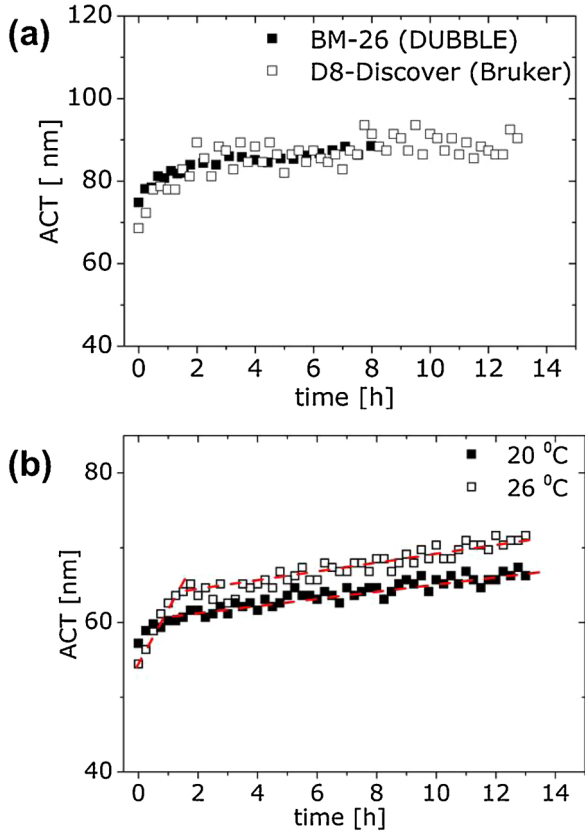

Fig. 7. (a) A comparison of the ACT data as a function of time obtained at the BM-26 (DUBBLE) beamline at ESRF (solid symbols) and at the lab-scale X-ray diffractometer Bruker D8-Discover (empty symbols). Both experiments were done for MFC nanoplatelets dispersed in sunflower oil in the developed Couette geometry with serrated walls at an imposed shear rate of 0.1 s^{-1} and ambient temperatures. (b) ACT as a function of time for MFC nanoplatelets dispersed in bean oil at an imposed shear rate of 1 s^{-1} and temperatures of 20 °C (solid symbols) and 26 °C (empty symbols). The measurements were performed in a rheo-SAXS Couette cell geometry (1 mm gap) at the D8-Discover.

and margarine, are defined by the underlying multiscale structure of fat crystal networks [7]. A novel route to design the fat crystal structure is based on dispersing micronized fat crystal (MFC) nanoplatelets in oil [41,10]. In this way, the crystallisation of the fat crystal nanoplatelets can be decoupled from the aggregation of fat crystals into larger structures, which could radically simplify manufacturing of food manufacturing routes. However, rational design of these routes is challenging, since kinetics of multiscale network formation is strongly determined by temperature and shear [42]. The developed shear cell was employed to assess kinetics of fat crystal mesoscale networks in well-controlled shear stress fields at different temperatures [10,46].

Fig. 6(a) shows the 2D SAXS pattern and an radial integration of the first order diffraction peak obtained under imposed shear 0.1 s^{-1} at the BM-26 (DUBBLE) beamline at ESRF. The rheo-SAXS experiment revealed the alignment of the dispersed MFC nanoplatelets under shear. As most of the information about individual MFC nanoplatelets lies in the first diffraction peak at scattering vectors $q = 1.6\,nm^{-1}$, it was also possible to perform experiments at a lab-scale X-ray diffractometer Bruker D8-Discover (A.12). Even though the obtained 2D pattern (Fig. 6(b)) had a different signal to noise ratio, the effect of shear on the alignment of MFC nanoplatelets could clearly be observed.

The presence of a well resolved first order diffraction peak allowed real-time assessment of the increase in average crystal thickness (ACT) of the dispersed MFC nanoplatelets under shear. The ACT was estimated based on the Scherrer line shape analysis [43,10]. Fig. 7(a) shows the ACT as a function of time under imposed constant shear of 0.1 s^{-1} at ambient temperature. The scattering patterns were obtained at the BM-26 (DUBBLE) beamline at ESRF. The increase in ACT during 8–13 h of shear points toward shear induced recrystallisation of the MFC nanoplatelets. This recrystallisation effect was also observed in a shear-SAXS experiment at D8-Discover diffractometer, albeit with lower signal to noise ratio (see Fig. 7(a)).

The performance of the variable temperature capability of the shear cell is illustrated by Fig. 7(b). MFC dispersions were measured at 20 and 26 °C with the shear cell mounted in a lab scale Discover D8 diffractometer for 13 h under constant shear of 1 s^{-1}. Even with this lab scale instrument kinetic curves could be obtained that allow observation of two recrystallisation stages of which one is clearly temperature dependent (see Fig. 7(b)) [10,46]. The availability of the rheo-SAXS cell with variable temperature capability which can versatile be mounted in both synchrotron beamlines and labscale instruments has been an

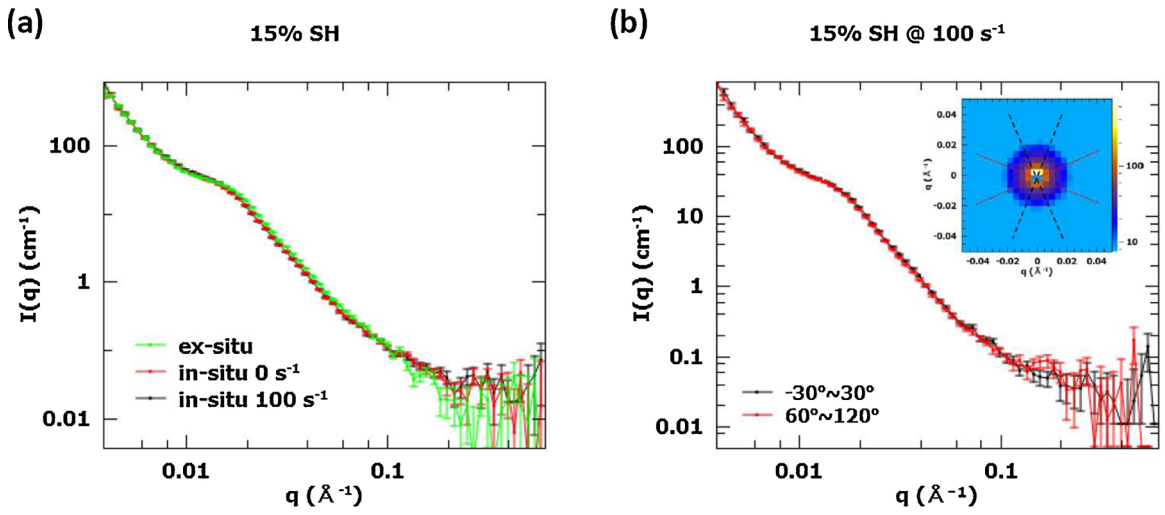

Fig. 8. Scattering patterns of 15% (w/w) calcium caseinate dissolved in H_2O (SH). (a) 1D scattering patterns of the sample sheared at 0, 100 $^{-1}$ and ex-situ; (b) intensities of sector-cut from the 2D patterns of the sample sheared at 100 $^{-1}$ (inset).

important enabler of studies investigated fat crystal network formation [10,46]. In future work we expect that the cell will also be deployed in combination with ultra small angle X-rays scattering (USAXS) to provide unprecedented views on network formation in the micronscale domain.

3.3. Neutrons: protein dispersions

Manski et al. [44] found a way to produce fibrous structure from calcium caseinate dispersion by applying simple shear, heat and enzyme transglutaminase. In order to investigate the structuring of calcium caseinate dispersions under shear, we have designed and performed a small-angle neutron scattering experiment [47]. The experiment was conducted at the LARMOR instrument at ISIS.

Fig. 8a shows the typical scattering patterns of the sample. All data were reduced with their corresponding background, for the shear-cell, the background is the cell filled with H_2O. A nearly perfect overlap between the sample measured ex-situ and at $0\,s^{-1}$ inside the shear-cell confirmed the shear-cell did not interfere with the sample. Surprisingly, the scattering pattern obtained at a shear rate as high as $100\,s^{-1}$ also overlapped perfectly with the others, indicating shear had no influence on the sample structure at the length scale studied. Moreover, the scattering is isotropic at all shear rates, as the radially averaged scattering intensity in Fig. 8b shows.

4. Conclusions

We have designed and built a versatile compact shear cell to perform SAXS, SANS and SESANS measurements with temperature control. The experimental section of the article has shown applications of the designed shear cell in studies of food materials. Each of the obtained results provides a valuable insight into structuring of the soft matter under shear, relevant to both fundamental and applied sciences.

Conflict of interest

There are no conflicts of interest, i.e., no financial or personal relationships with other people or organizations that could inappropriately influence this work.

Acknowledgements

We thank Gerrit W.M. Peters (Department of Mechanical Engineering Materials Technology Institute, Eindhoven University of Technology) and Wim Bras (DUBBLE CRG BM26@ESRF, Netherlands Organization for Scientific Research (NWO), European Synchrotron Radiation Facility) for their contribution in the design of the shear cell, Ruud den Adel and Adrian Voda (Unilever R&D Vlaardingen) for their help and technical assistance with the testing of the shear cell and temperature shell with the Bruker D8-Discover diffractometer, Daniel Hermida Merino (DUBBLE CRG BM26@ESRF, Netherlands Organization for Scientific Research (NWO), European Synchrotron Radiation Facility), Robert Dalgliesh and Adam Washington (LARMOR beamline, ISIS neutron and muon source) for their help and technical assistance during SAXS and SANS experiments, respectively, Netherlands Organization for Scientific Research (NWO) and NWO Domain Applied and Engineering Sciences (AES) for giving us opportunity to perform SAXS experiments at DUBBLE beamline, and Ernst van der Waals (DEMO, TU Delft) for his help and technical assistance with the development of the shear cell and temperature shell. This work is part of the research program Open Technology with project number 13386 which is financed by the Netherlands Organization for Scientific Research (NWO).

Appendix A. Supplementary data

Supplementary data associated with this article can be found, in the online version, at https://doi.org/10.1016/j.colsurfa.2018.12.046.

References

[1] A.J. van der Goot, P.J. Pelgrom, J.A. Berghout, M.E. Geerts, L. Jankowiak, N.A. Hardt, J. Keijer, M.A. Schutyser, C.V. Nikiforidis, R.M. Boom, Concepts for further sustainable production of foods, J. Food Eng. 168 (2016) 42–51, https://doi.org/10.1016/j.jfoodeng.2015.07.010.
[2] M.A. Augustin, M. Riley, R. Stockmann, L. Bennett, A. Kahl, T. Lockett, M. Osmond, P. Sanguansri, W. Stonehouse, I. Zajac, L. Cobiac, Role of food processing in food and nutrition security, Trends Food Sci. Technol. 56 (2016) 115–125, https://doi.org/10.1016/j.tifs.2016.08.005.
[3] J. Ubbink, Soft matter approaches to structured foods: from “cook-and-look” to rational food design? Faraday Discuss. 158 (2012) 9, https://doi.org/10.1039/c2fd20125a.
[4] R. Mezzenga, P. Schurtenberger, A. Burbidge, M. Michel, Understanding foods as soft materials, Nat. Mater. 4 (10) (2005) 729–740, https://doi.org/10.1038/nmat1496.
[5] J. Doutch, E.P. Gilbert, Characterisation of large scale structures in starch granules via small-angle neutron and X-ray scattering, Carbohydr. Polym. 91 (1) (2013) 444–451, https://doi.org/10.1016/j.carbpol.2012.08.002.
[6] A. Lopez-Rubio, B.M. Flanagan, A.K. Shrestha, M.J. Gidley, E.P. Gilbert, Molecular rearrangement of starch during in vitro digestion: toward a better understanding of enzyme resistant starch formation in processed starches, Biomacromolecules 9 (7) (2008) 1951–1958, https://doi.org/10.1021/bm800213h.
[7] P.R.R. Ramel, F. Peyronel, A.G. Marangoni, Characterization of the nanoscale structure of milk fat, Food Chem. 203 (2016) 224–230, https://doi.org/10.1016/j.foodchem.2016.02.064.
[8] F. Peyronel, B. Quinn, A.G. Marangoni, D.a. Pink, Ultra small angle X-ray scattering in complex mixtures of triacylglycerols, J. Phys.: Condens. Matter 26 (46) (2014) 464110, https://doi.org/10.1088/0953-8984/26/46/464110.
[9] M. Nieuwland, W.G. Bouwman, M.L. Bennink, E. Silletti, H.H.J. de Jongh, Characterizing length scales that determine the mechanical behavior of gels from crosslinked casein micelles, Food Biophys. (2015), https://doi.org/10.1007/s11483-015-9399-y.
[10] T. Nikolaeva, R. den Adel, E. Velichko, W.G. Bouwman, D. Hermida-Merino, H. Van As, A. Voda, J. van Duynhoven, Networks of micronized fat crystals grown under static conditions, Food Funct. 9 (4) (2018) 2102–2111, https://doi.org/10.1039/C8FO00148K.
[11] J. Vermant, M.J. Solomon, Flow-induced structure in colloidal suspensions, J. Phys.: Condens. Matter 17 (4) (2005) R187–R216, https://doi.org/10.1088/0953-8984/17/4/R02.
[12] A.P.R. Eberle, L. Porcar, Flow-SANS and rheo-SANS applied to soft matter, Curr. Opin.Colloid Interface Sci. 17 (1) (2012) 33–43, https://doi.org/10.1016/j.cocis.2011.12.001.
[13] A. Lopez-Rubio, E.P. Gilbert, Neutron scattering: a natural tool for food science and technology research, Trends Food Sci. Technol. 20 (11-12) (2009) 576–586, https://doi.org/10.1016/j.tifs.2009.07.008.
[14] M.T. Rekveldt, J. Plomp, W.G. Bouwman, W.H. Kraan, S. Grigoriev, M. Blaauw, Spin-echo small angle neutron scattering in Delft, Rev. Sci. Instrum. 76 (3) (2005) 033901, https://doi.org/10.1063/1.1858579.
[15] P. Panine, M. Gradzielski, T. Narayanan, Combined rheometry and small-angle X-ray scattering, Rev. Sci. Instrum. 74 (4) (2003) 2451–2455, https://doi.org/10.1063/1.1556943.
[16] J. Stellbrink, B. Lonetti, G. Rother, L. Willner, D. Richter, Shear induced structures of soft colloids: rheo-SANS experiments on kinetically frozen PEP-PEO diblock copolymer micelles, J. Phys.: Condens. Matter 20 (40) (2008) 404206, https://doi.org/10.1088/0953-8984/20/40/404206.
[17] M.W. Liberatore, F. Nettesheim, N.J. Wagner, L. Porcar, Spatially resolved small-angle neutron scattering in the 1–2 plane: a study of shear-induced phase-separating wormlike micelles, Phys. Rev. E 73 (2) (2006) 020504, https://doi.org/10.1103/PhysRevE.73.020504.
[18] A.K. Gurnon, P.D. Godfrin, N.J. Wagner, A.P.R. Eberle, P. Butler, L. Porcar, Measuring material microstructure under flow using 1–2 plane flow-small angle neutron scattering, J. Vis. Exp. 84 (February) (2014) 51068, https://doi.org/10.3791/51068.
[19] M.W. Liberatore, F. Nettesheim, P.A. Vasquez, M.E. Helgeson, N.J. Wagner, E.W. Kaler, L.P. Cook, L. Porcar, Y.T. Hu, Microstructure and shear rheology of entangled wormlike micelles in solution, J. Rheol. 53 (2) (2009) 441–458, https://doi.org/10.1122/1.3072077.
[20] M.E. Helgeson, M.D. Reichert, Y.T. Hu, N.J. Wagner, Relating shear banding, structure, and phase behavior in wormlike micellar solutions, Soft Matter 5 (20) (2009) 3858, https://doi.org/10.1039/b900948e.
[21] M.E. Helgeson, L. Porcar, C. Lopez-Barron, N.J. Wagner, Direct observation of flow-concentration coupling in a shear-banding fluid, Phys. Rev. Lett. 105 (8) (2010) 084501, https://doi.org/10.1103/PhysRevLett.105.084501.
[22] K.M. Weigandt, L. Porcar, D.C. Pozzo, In situ neutron scattering study of structural transitions in fibrin networks under shear deformation, Soft Matter 7 (21) (2011) 9992, https://doi.org/10.1039/c1sm06176c.
[23] P. Lindner, R. Oberth“ur, Apparatus for the investigation of liquid systems in a shear gradient by small angle neutron scattering (SANS), Revue de Physique

Appliquée 19 (9) (1984) 759–763, https://doi.org/10.1051/rphysap:0198400190907590.
[24] G.C. Straty, Apparatus for neutron scattering measurements, J. Res. Natl. Inst. Stand. Technol. Apparatus 94 (4) (1989) 259–261.
[25] P.G. Cummins, E. Staple, B.J.P. Millen, A Couette shear flow cell for small-angle neutron scattering studies, Meas. Sci. Technol. 1 (2) (1990) 179–183.
[26] G.C. Straty, H.J.M. Hanley, C.J. Glinka, Shearing apparatus for neutron scattering studies on fluids: preliminary results for colloidal suspensions, J. Stat. Phys. 62 (5–6) (1991) 1015–1023, https://doi.org/10.1007/BF01128174.
[27] S. Okamoto, K. Saijo, T. Hashimoto, Dynamic SAXS studies of sphere-forming block copolymers under large oscillatory shear deformation, Macromolecules 27 (14) (1994) 3753–3758, https://doi.org/10.1021/ma00092a012.
[28] S.M. Baker, G. Smith, R. Pynn, P. Butler, J. Hayter, W. Hamilton, L. Magid, Shear cell for the study of liquid–solid interfaces by neutron scattering, Rev. Sci. Instrum. 65 (2) (1994) 412–416, https://doi.org/10.1063/1.1145148.
[29] L. Noirez, A. Lapp, Shear flow induced transition from liquid-crystalline to polymer behavior in side-chain liquid crystal polymers, Phys. Rev. Lett. 78 (1) (1997) 70–73, https://doi.org/10.1103/PhysRevLett.78.70.
[30] C. Dux, S. Musa, V. Reus, H. Versmold, D. Schwahn, P. Lindner, Small angle neutron scattering experiments from colloidal dispersions at rest and under sheared conditions, J. Chem. Phys. 109 (6) (1998) 2556–2561, https://doi.org/10.1063/1.476828.
[31] F. Molino, J.-F. Berret, G. Porte, O. Diat, P. Lindner, Identification of flow mechanisms for a soft crystal, Eur. Phys. J. B 3 (1) (1998) 59–72, https://doi.org/10.1007/s100510050284.
[32] F.E. Caputo, W.R. Burghardt, Real-time 1–2 plane SAXS measurements of molecular orientation in sheared liquid crystalline polymers, Macromolecules 34 (19) (2001) 6684–6694, https://doi.org/10.1021/ma0107556.
[33] L. Porcar, W.A. Hamilton, P.D. Butler, G.G. Warr, A vapor barrier Couette shear cell for small angle neutron scattering measurements, Rev. Sci. Instrum. 73 (6) (2002) 2345–2354, https://doi.org/10.1063/1.1475351.
[34] B. Struth, K. Hyun, E. Kats, T. Meins, M. Walther, M. Wilhelm, G. Gr”ubel, Observation of new states of liquid crystal 8CB under nonlinear shear conditions as observed via a novel and unique rheology/small-angle X-ray scattering combination, Langmuir 27 (6) (2011) 2880–2887, https://doi.org/10.1021/la103786w.
[35] L. Porcar, D. Pozzo, G. Langenbucher, J. Moyer, P.D. Butler, Rheo-small-angle neutron scattering at the National Institute of Standards and Technology Center for Neutron Research, Rev. Sci. Instrum. 82 (8) (2011) 083902, https://doi.org/10.1063/1.3609863.
[36] P. Pfleiderer, S.J. Baik, Z. Zhang, G. Vleminckx, M.P. Lettinga, E. Grelet, J. Vermant, C. Clasen, X-ray scattering in the vorticity direction and rheometry from confined fluids, Rev. Sci. Instrum. 85 (6) (2014) 065108, https://doi.org/10.1063/1.4881796.
[37] J.J. Richards, N.J. Wagner, P.D. Butler, A strain-controlled RheoSANS instrument for the measurement of the microstructural, electrical, and mechanical properties of soft materials, Rev. Sci. Instrum. 88 (10) (2017) 105115, https://doi.org/10.1063/1.4986770.
[38] M. Borsboom, W. Bras, I. Cerjak, D. Detollenaere, D. Glastra van Loon, P. Goedtkindt, M. Konijnenburg, P. Lassing, Y.K. Levine, B. Munneke, M. Oversluizen, R. van Tol, E. Vlieg, The Dutch–Belgian beamline at the ESRF, J. Synchrontron Radiat. 5 (3) (1998) 518–520, https://doi.org/10.1107/S0909049597013484.
[39] W. Bras, I. Dolbnya, D. Detollenaere, R. van Tol, M. Malfois, G. Greaves, A. Ryan, E. Heeley, Recent experiments on a small-angle/wide-angle X-ray scattering beam line at the ESRF, J. Appl. Crystallogr. 36 (3) (2003) 791–794, https://doi.org/10.1107/S002188980300400X.
[40] D. de Kort, S. Veen, H. Van As, D. Bonn, K. Velikov, J. van Duynhoven, Yielding and flow of cellulose microfibril dispersions in the presence of a charged polymer, Soft Matter (2016), https://doi.org/10.1039/c1sm05495c.
[41] P. M“un”uklü, P. Jansens, Particle formation of an edible fat (rapeseed 70) using the supercritical melt micronization (ScMM) process, J. Supercrit. Fluids 40 (3) (2007) 433–442, https://doi.org/10.1016/j.supflu.2006.07.015.
[42] F. Maleky, G. Mazzanti, Lipid crystal networks structured under shear flow, Crystallization of Lipids, John Wiley & Sons, Ltd., Chichester, UK, 2018, pp. 211–239, https://doi.org/10.1002/9781118593882.ch7.
[43] R. den Adel, K. van Malssen, J. van Duynhoven, O.O. Mykhaylyk, A. Voda, Fat crystallite thickness distribution based on SAXD peak shape analysis, Eur. J. Lipid Sci. Technol. 120 (9) (2018) 1800222, https://doi.org/10.1002/ejlt.201800222.
[44] J.M. Manski, A.J. van der Goot, R.M. Boom, Advances in structure formation of anisotropic protein-rich foods through novel processing concepts, Trends Food Sci. Technol. 18 (11) (2007) 546–557, https://doi.org/10.1016/j.tifs.2007.05.002.
[45] E. Velichko, et al. (to be published).
[46] T. Nikolaeva, R. den Adel, R. van der Sman, K.J.A. Martens, H. Van As, A. Voda, J. van Duynhoven, Manipulation of recrystallisation and network formation of oil-dispersed micronized fat crystals (submitted for publication).
[47] B. Tian, et al. (to be published).